Phase transition of $BaTiO_3$–$Ba_{1-x}Pb_xTiO_3$ composite particles prepared by the molten salt method

Yoshiho Ito, Shiro Shimada, Jun-ichi Takahashi and Michio Inagaki

Division of Materials Science and Engineering, Graduate School of Engineering, Hokkaido University 8-West, 13-North, Kita-ku, Sapporo, 060 Japan

$BaTiO_3$–$Ba_{1-x}Pb_xTiO_3$ composite particles have been prepared by the molten salt reaction at 600 °C in the $BaTiO_3$–$PbCl_2$ system. A coating of $Ba_{1-x}Pb_xTiO_3$ on $BaTiO_3$ was indicated by X-ray diffraction (XRD), high-temperature XRD (HTXRD) and energy-dispersive X-ray analysis (EDXA). Different particle sizes of $BaTiO_3$ (0.1 μm and 0.5 μm) and molar ratios of $PbCl_2/BaTiO_3$ (0.5 and 1.0) produced two sizes of composite particles, the larger particles having estimated x values of $0.5 \leqslant x \leqslant 0.8$ and $x \approx 0.9$, and the smaller particles having x values of $0.4 \leqslant x \leqslant 1.0$. The phase transition was followed by HTXRD and differential scanning calorimetry (DSC) measurements during heating and cooling. The results of dielectric measurements were used to provide an explanation of the phase transition in the composite particles.

Barium titanate ($BaTiO_3$) is widely used as a capacitor material with a high relative permittivity (ε) at room temperature.[1] It undergoes a phase transition from tetragonal to cubic at 130 °C on heating and reveals a sharp anomaly in the temperature dependence of the relative permittivity [$\varepsilon(T)$]. For the use of $BaTiO_3$ as a capacitor, a high relative permittivity with good temperature stability is required at the working temperature. These properties have been achieved by the addition of other elements such as Bi_2O_3, Nb_2O_5 and CdO which shift the Curie temperature (T_c) from 130 °C to room temperature and flatten the shape of the Curie peak, leading to some $BaTiO_3$-related ceramics with X7R behaviour. Such ceramics show temperature-stable dielectric characteristics of the X7R type, depending on the volume fraction of the chemical inhomogeneity and also on the stress induced by the difference in unit cell volume between the core and shell of the grain.[2–4] The working temperature in these ceramics is within ±100 °C of room temperature. Recent increases in the demand for high-temperature capacitors have necessitated the development of improved dielectric materials. For such capacitors to be developed, dielectric materials with high temperature stability need to be fabricated.

A solid solution of $Ba_{1-x}Pb_xTiO_3$ is an attractive material for such applications, since T_c can be controlled by the x value, and the relative permittivity is high.[5] We have previously reported that $Ba_{1-x}Pb_xTiO_3$ solid solutions of fixed composition x can be prepared by a molten salt reaction between $BaTiO_3$ powders and molten $PbCl_2$ at relatively low temperatures ($\leqslant$600 °C); this is referred to as a soft process because of the low synthesis temperature.[6] Since the molten salt reaction leads to substitution of Pb^{2+} for Ba^{2+} in solid $BaTiO_3$, partial substitution under appropriate conditions may leave some unreacted $BaTiO_3$. With a low $PbCl_2/BaTiO_3$ ratio ($\leqslant$0.7) and/or large $BaTiO_3$ particles (0.5 μm), powders containing both $Ba_{1-x}Pb_xTiO_3$ and $BaTiO_3$ could be formed.[6] When a partial reaction of a sintered $BaTiO_3$ bulk compact with molten $PbCl_2$ was carried out, a double structured composite body with an inner core of $BaTiO_3$ and an outer shell of $Ba_{1-x}Pb_xTiO_3$ was produced, in which compositional gradients of Ba and Pb existed between the two phases.[7] It is thus worth examining whether or not particles containing two phases, $Ba_{1-x}Pb_xTiO_3$ and $BaTiO_3$, possess a double structure (core–shell structure) similar to the sintered compact. If core–shell particles consisting of ferroelectric $Ba_{1-x}Pb_xTiO_3$ covering ferroelectric or paraelectric $BaTiO_3$ are formed, an interesting dielectric property, different from that of the $BaTiO_3$-based X7R type ceramics, would be developed.

The present work describes the formation of composite particles of $BaTiO_3$–$Ba_{1-x}Pb_xTiO_3$ with variable x values by the molten salt reaction between $BaTiO_3$ and $PbCl_2$, using different particle sizes of $BaTiO_3$ and different mole ratios. A comparison of the phase transition of the composite particles with that of a single-phase $Ba_{1-x}Pb_xTiO_3$ solid solution was made on the basis of high-temperature X-ray diffraction (HTXRD) and differential scanning calorimetry (DSC) results. Since the relationship between the transition temperature and the composition has been reported for the solid solution of $Ba_{1-x}Pb_xTiO_3$,[1] the compositions of the composite particles obtained were also estimated from this relationship. The dielectric properties of sintered compacts fabricated from synthesized $BaTiO_3$–$Ba_{1-x}Pb_xTiO_3$ powders were measured.

Experimental

Reagents and preparation

$Ba_{1-x}Pb_xTiO_3$ and $BaTiO_3$–$Ba_{1-x}Pb_xTiO_3$ powders were prepared by the molten salt method in the system $BaTiO_3$–$PbCl_2$ as reported previously.[3] The starting materials were two hydrothermally synthesized $BaTiO_3$ powders with average particle sizes of 0.1 and 0.5 μm (99.97 and 99.94% purity, respectively; Murata Manufacturing Co., Japan), and a reagent-grade $PbCl_2$ powder (99% pure; Kishida Chemicals, Japan). The 0.1 and 0.5 μm $BaTiO_3$ powders have cubic and tetragonal structures, respectively, as determined by XRD at room temperature. The $BaTiO_3$ and $PbCl_2$ powders were well mixed in a mole ratio of 0.5 to 1.0 and heated in a platinum crucible with a tight lid at 600 °C for 100–240 h under a nitrogen atmosphere. The reaction conditions are summarized in Table 1. After reaction, the chlorides remaining in the product were removed by repeated treatment with dilute nitric acid solution (0.5 mol dm^{-3}) and distilled water until no Cl^- in the washed solution was detected by $AgNO_3$. The washed products were dried on a hot plate at 100 °C.

Characterization

Phase identification was performed by XRD with Cu-Kα radiation at room temperature. The product was dissolved in hot phosphoric acid, and the amounts of barium and lead in the solution were quantitatively determined by inductively coupled plasma (ICP) spectrometry. The morphology and

Table 1 Molten salt reaction in the system $BaTiO_3$–$PbCl_2$ at 600 °C

sample	particle size of starting $BaTiO_3$/μm	$PbCl_2/BaTiO_3$ molar ratio	reaction time/h	product[a]
A	0.1	1.0	100	single phase (tetra. $Ba_{0.13}Pb_{0.87}TiO_3$ solid solution)
B	0.5	1.0	240	two phases (tetra. $BaTiO_3$ and tetra. $Ba_{1-x}Pb_xTiO_3$)
C	0.1	0.5	100	two phases (cubic $BaTiO_3$ and tetra. $Ba_{1-x}Pb_xTiO_3$)

[a]tetra. means tetragonal.

composition of the particles were examined by TEM at an accelerating voltage of 200 kV, with EDXA.

Phase transition

The phase transition of the synthesized composite powder product was monitored by HTXRD with Cu-Kα radiation at fixed temperatures between 25 and 550 °C during heating and cooling cycles, using a stainless-steel sample holder. The HTXRD measurements were made on samples equilibrated at each temperature for more than 1 h.

DSC was also carried out on the sample powders, which were packed in a Au-coated Ag cell, during heating and cooling cycles at a rate of 10 °C min^{-1} between 25 and 600 °C. Reagent-grade Al_2O_3 powder was used as the reference.

Dielectric measurements

Two $BaTiO_3$–$Ba_{1-x}Pb_xTiO_3$ powders with different x values were uniaxially compressed into disks of diameter 12 mm and thickness 2 mm under a pressure of 50 MPa, followed by cold isostatic pressing (CIP) at 400 MPa. The disk was buried in a powder of the same composition, and heated to 800–900 °C in static air. Silver electrodes were coated on both sides of the sintered compact and fired at 575 °C for 10 min. The dielectric properties of the compacts were measured at temperatures in the range 25–600 °C at frequencies of 1, 10 and 100 kHz using an inductance–capacitance–resistance (LCR) meter.

Results and Discussion

Structure and composition of the product

Fig. 1 shows the XRD profiles at 42–47° (2θ) of three types of particles prepared by reaction of $BaTiO_3$ with molten $PbCl_2$ at 600 °C. The three types of particles, labelled as samples A, B and C, are summarized in Table 1. Using 0.1 μm $BaTiO_3$ and a mole ratio ($PbCl_2/BaTiO_3$) of 1.0, the product powders (sample A) contain a single-phase tetragonal perovskite solid solution [Fig. 1(A)] of composition $Ba_{0.13}Pb_{0.87}TiO_3$ as determined by ICP analysis. The peaks corresponding to the 002 and 200 reflections of the tetragonal perovskite were relatively narrow compared with the other two products, suggesting a narrow composition distribution.

Reaction of 0.5 μm $BaTiO_3$ and $PbCl_2$ with a molar ratio of 1.0 gave powders (sample B) containing two tetragonal phases of $BaTiO_3$ and $Ba_{1-x}Pb_xTiO_3$ [Fig. 1(B)] with a Pb/(Pb + Ba) ratio of 0.46, since the 002 and 200 reflections of the tetragonal $BaTiO_3$ and $Ba_{1-x}Pb_xTiO_3$ appear. The diffraction position of $BaTiO_3$ was virtually identical to that of pure $BaTiO_3$. The two $Ba_{1-x}Pb_xTiO_3$ peaks were relatively broad and close together, compared with those of the single-phase solid solution, suggesting that $Ba_{1-x}Pb_xTiO_3$ has a wide compositional distribution with x values less than 0.87, as found for the single-phase solid solution.

Reaction of 0.1 μm $BaTiO_3$ and $PbCl_2$ with a molar ratio of 0.5 produced two phases (sample C), cubic $BaTiO_3$ and tetragonal $Ba_{1-x}Pb_xTiO_3$ [Fig. 1(C)]. The Pb/(Pb + Ba) ratio was determined as 0.46, as in $BaTiO_3$–$Ba_{1-x}Pb_xTiO_3$ derived from 0.5 μm $BaTiO_3$. Since the two diffraction peaks of

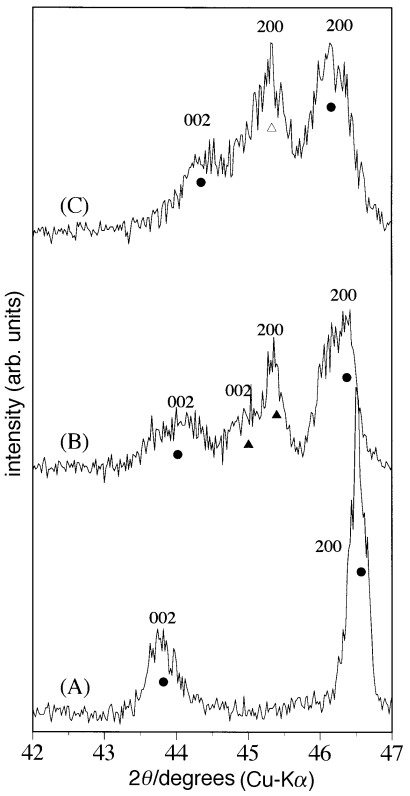

Fig. 1 XRD patterns for the 002 and 200 reflections of (A) the solid solution particles of $Ba_{0.13}Pb_{0.87}TiO_3$, (B) large composite particles of $BaTiO_3$–$Ba_{1-x}Pb_xTiO_3$, and (C) small composite particles of $BaTiO_3$–$Ba_{1-x}Pb_xTiO_3$. $BaTiO_3$: tetragonal, ▲; cubic, △. $Ba_{1-x}Pb_xTiO_3$: tetragonal, ●.

$Ba_{1-x}Pb_xTiO_3$ were broader and closer together than those in Fig. 1(B), this phase is thought to have a wider compositional distribution and a smaller x value in $Ba_{1-x}Pb_xTiO_3$ than that obtained for 0.5 μm $BaTiO_3$.

The TEM images of the three powder products are shown in Fig. 2. The particles of the $Ba_{0.13}Pb_{0.87}TiO_3$ solid solution [sample A; Fig. 2(A)] are larger than the original cubic perovskite $BaTiO_3$ particles [Fig. 2(D)]. EDXA showed no compositional differences between the solid solution particles.

The particles of sample B are of almost uniform size of about 0.7 μm [Fig. 2(B)], which is larger than the particle size of the starting material [Fig. 2(E)]. EDXA showed that the Pb/(Pb + Ba) ratios at the edges of the composite particles range from 0.68 to 0.87, while the ratio near the centre was 0.14–0.55. Pure $BaTiO_3$ particles were not found by TEM–EDXA, but the particles examined were found to always contain Ba and Pb. The XRD patterns of sample B showed the coexistence of $Ba_{1-x}Pb_xTiO_3$ and $BaTiO_3$ phases. Therefore, it is suggested that pure $BaTiO_3$ and $Ba_{1-x}Pb_xTiO_3$ coexisted in the particles of sample B to form composite particles of $BaTiO_3$–$Ba_{1-x}Pb_xTiO_3$, probably consisting of $BaTiO_3$ covered with $Ba_{1-x}Pb_xTiO_3$. The Pb/(Pb + Ba) ratios

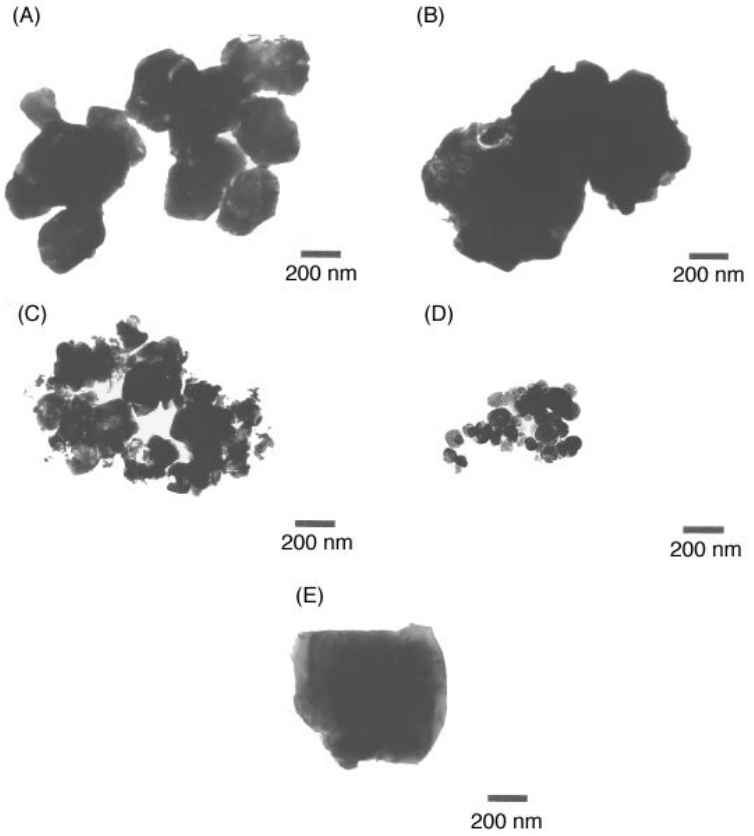

Fig. 2 TEM images of (A) particles of $Ba_{0.13}Pb_{0.87}TiO_3$ solid solution, (B) large composite particles of $BaTiO_3$–$Ba_{1-x}Pb_xTiO_3$, (C) small composite particles of $BaTiO_3$–$Ba_{1-x}Pb_xTiO_3$, (D) 0.1 μm $BaTiO_3$ reactant particles and (E) 0.5 μm $BaTiO_3$ reactant particles

at the edges were comparable to those of $Ba_{1-x}Pb_xTiO_3$ determined from the XRD results [Fig. 1(B)].

The particles of sample C [Fig. 2(C)] are also larger (0.3 μm) than the starting grains (0.1 μm) [Fig. 2(D)]. An EDXA indicated Pb/(Pb + Ba) ratios of 0.54–0.84 at the particle edges and 0.40–0.79 near the centre; the Pb/(Pb + Ba) ratios at the edge and centre were not greatly different in the small particles prepared from 0.1 μm $BaTiO_3$, probably because of the limiting electron probe size. As in the case of sample B, pure $BaTiO_3$ particles were not found, but the particles were found to contain Ba and Pb (by EDXA). These results and the coexistence of $BaTiO_3$–$Ba_{1-x}Pb_xTiO_3$ phases [Fig. 1(C)] suggest that composite particles consisting of cubic $BaTiO_3$ covered with tetragonal $Ba_{1-x}Pb_xTiO_3$ with various x values are produced. It is understood that these composite particles in both samples B and C consist of an inner core of $BaTiO_3$ and an outer shell of $Ba_{1-x}Pb_xTiO_3$, although direct evidence of the core–shell structure cannot be obtained at present.

Phase transition

Fig. 3(A) shows the HTXRD patterns for the 002 and 200 reflections of the $Ba_{0.13}Pb_{0.87}TiO_3$ solid solution (sample A) during heating to 500 °C. The separation between the 002 and 200 peaks decreases with increasing temperature, and the peaks finally merge at 480 °C owing to the phase transition from the tetragonal (t) to the cubic (c) structure.

The composite $BaTiO_3$–$Ba_{1-x}Pb_xTiO_3$ particles of 0.7 μm size (sample B) show more complicated phase transitions [Fig. 3(B)]. The tetragonal to cubic phase change of the $BaTiO_3$ core takes place at 130 °C. The 002 and 200 peaks corresponding to the tetragonal $Ba_{1-x}Pb_xTiO_3$ shell similarly approach each other with increasing temperature [Fig. 3(B)]. The 200 peak of cubic $Ba_{1-x}Pb_xTiO_3$ begins to appear around 45.3° at 400 °C in addition to tetragonal $Ba_{1-x}Pb_xTiO_3$ and becomes strong with increasing temperature, in contrast to the tetragonal 200 peak which decreases and disappears at 480 °C. The cubic 200 peak intensity of $Ba_{1-x}Pb_xTiO_3$ was almost the same as that of $BaTiO_3$ at 550 °C. The coexistence of cubic and tetragonal $Ba_{1-x}Pb_xTiO_3$ phases suggests the presence of $Ba_{1-x}Pb_xTiO_3$ coated particles having various x values over a wide range.

The phase transition of the small (0.3 μm) particles of the $BaTiO_3$–$Ba_{1-x}Pb_xTiO_3$ composite (sample C) is shown in Fig. 3(C). The inner $BaTiO_3$ core of the composite particles remains cubic during heating to 550 °C. The 002 and 200 peaks corresponding to the covering tetragonal $Ba_{1-x}Pb_xTiO_3$ shell approach each other with increasing temperature and are hardly visible at 480 °C. A hump around 45.3° at 360–400 °C grows into a peak at 440–550 °C. This peak, which represents the 200 peak of cubic $Ba_{1-x}Pb_xTiO_3$, grows from the tetragonal phase, and increases with increasing temperature to attain almost the same intensity as that of $BaTiO_3$ at 500–550 °C.

Fig. 4 shows DSC curves for the three types of particles. The $Ba_{0.13}Pb_{0.87}TiO_3$ solid solution shows only one endotherm at 480 °C, consistent with the tetragonal (t)↔cubic (c) transition determined by HTXRD [Fig. 3(A)]. The DSC curve for sample B shows three minima at 140, 390 and 480 °C during heating [Fig. 4(B)]. According to HTXRD [Fig. 3(B)], the peak at 140 °C corresponds to the t↔c transition of the $BaTiO_3$ core, the broad peak which occurs over a wide temperature range (360–430 °C) and the sharp peak at 480 °C are associated with the t↔c transition of the covering $Ba_{1-x}Pb_xTiO_3$ shell. The DSC curve for sample C shows a very broad endotherm at 250–550 °C, with minima at 380 and 480 °C [Fig. 4(C)], consistent with the t↔c transition determined by HTXRD [Fig. 3(C)]. The HTXRD and DSC measurements on cooling the three types of samples were similar to the heating curves.

A comparison was made between the three types of particles, namely the $Ba_{0.13}Pb_{0.87}TiO_3$ solid solution (sample A), the large composite particles of $BaTiO_3$–$Ba_{1-x}Pb_xTiO_3$ (0.7 μm;

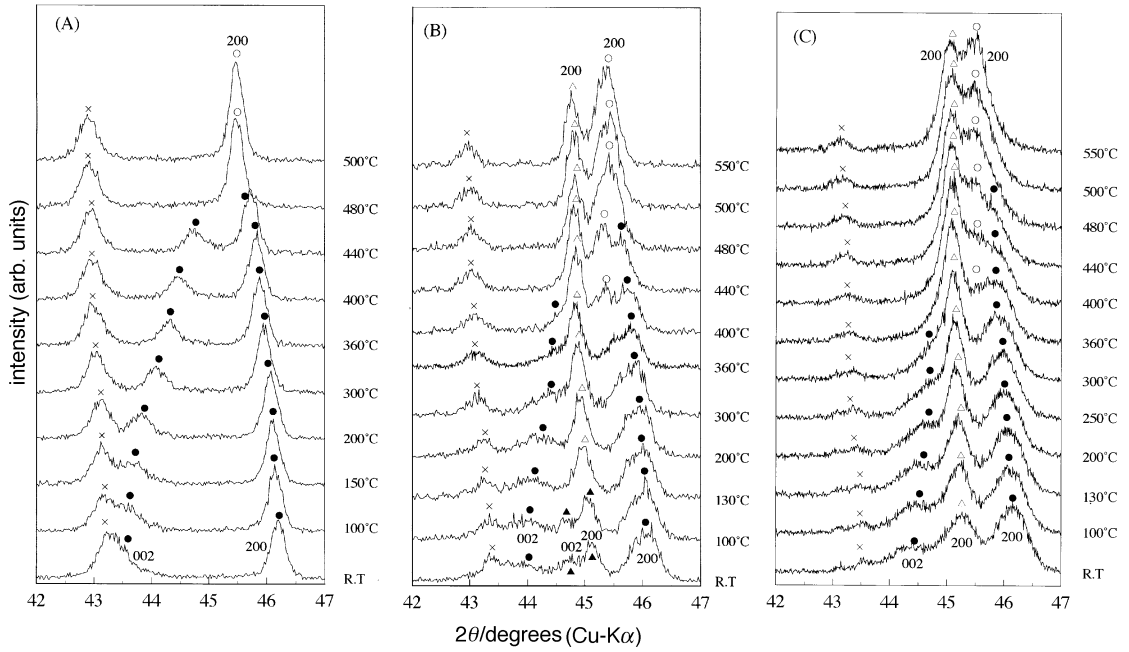

Fig. 3 HTXRD patterns for the 002 and 200 reflections of (A) the particles of the $Ba_{0.13}Pb_{0.87}TiO_3$ solid solution, (B) large composite particles of $BaTiO_3$–$Ba_{1-x}Pb_xTiO_3$ and (C) small composite particles of $BaTiO_3$–$Ba_{1-x}Pb_xTiO_3$ during heating to 550 °C. $BaTiO_3$: tetragonal, ▲; cubic, △. $Ba_{1-x}Pb_xTiO_3$: tetragonal, ●; cubic, ○. Reflections marked × are due to the stainless-steel sample holder.

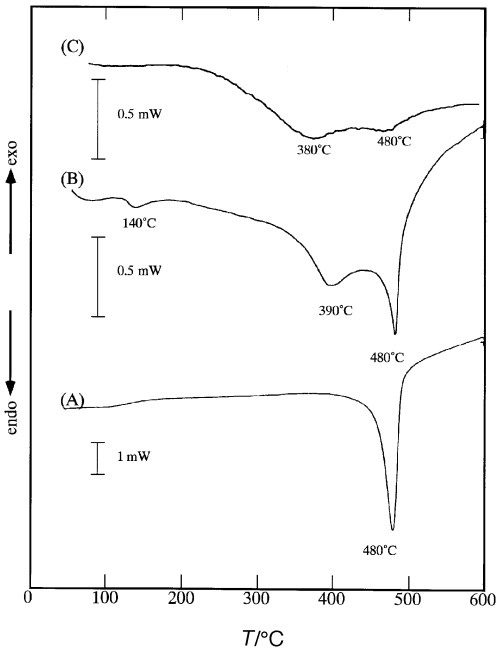

Fig. 4 DSC curves for (A) $Ba_{0.13}Pb_{0.87}TiO_3$ solid solution, (B) large composite particles of $BaTiO_3$–$Ba_{1-x}Pb_xTiO_3$, and (C) small composite particles of $BaTiO_3$–$Ba_{1-x}Pb_xTiO_3$; heating rate 10 °C min^{-1}

sample B) and the small composite particles of $BaTiO_3$–$Ba_{1-x}Pb_xTiO_3$ (0.3 μm; sample C). The single-phase $Ba_{0.13}Pb_{0.87}TiO_3$ solid solution showed the tetragonal to cubic phase transition at 480 °C (by HTXRD and DSC), in good agreement with the reported result.[1]

For the large composite particles, the t↔c transition of the covering $Ba_{1-x}Pb_xTiO_3$ shell [Fig. 3(B) and 4(B)] proceeded gradually over a temperature range of 360–430 °C and rapidly at 480 °C. This transition behaviour implies a wide distribution of x values in the $Ba_{1-x}Pb_xTiO_3$ shell, because the transition of $Ba_{1-x}Pb_xTiO_3$ with a fixed x value should take place at a fixed temperature. The two DSC endotherms suggest two different distributions of x values in the $Ba_{1-x}Pb_xTiO_3$ shell [Fig. 4(B)]. From the relationship between the transition temperature and the x value in $Ba_{1-x}Pb_xTiO_3$,[1] the x values of the present samples were estimated to be $0.5 \leqslant x \leqslant 0.8$ and $x \approx 0.9$, in good agreement with the Pb/(Pb + Ba) ratio determined by EDXA. It is assumed that $Ba_{1-x}Pb_xTiO_3$ with $0.5 \leqslant x \leqslant 0.8$ exists as an intermediate phase between the $BaTiO_3$ core and the outer Pb-rich $Ba_{0.1}Pb_{0.9}TiO_3$ shell in a composite particle (three phases in a particle), or that a $Ba_{1-x}Pb_xTiO_3$ shell with various x values covers the $BaTiO_3$ core (two phases in a particle). The area of the endotherm resulting from the t↔c transition of $BaTiO_3$ suggests that this $BaTiO_3$ occupies a considerable volume fraction (*ca.* ½) of the composite particle, since the enthalpy required for the t↔c transition is much smaller for pure $BaTiO_3$ (0.2 kJ mol^{-1}) than for pure $PbTiO_3$ (4.6 kJ mol^{-1}).[8]

The t↔c transition in the $Ba_{1-x}Pb_xTiO_3$ shell of the small composite particles (0.3 μm) proceeds continuously between 250 and 550 °C [Fig. 3(C) and 4(C)]. The x values in the $Ba_{1-x}Pb_xTiO_3$ shell are estimated to be $0.4 \leqslant x \leqslant 1.0$. It is suggested that either a wide concentration gradient exists in the $Ba_{1-x}Pb_xTiO_3$ shell of the composite particle or that the composite particles consist of a number of $BaTiO_3$–$Ba_{1-x}Pb_xTiO_3$ grains with a wide range of x values (two phases in a particle). Since the starting powders of 0.1 μm $BaTiO_3$ particles has the cubic phase, no transition occurs around 130 °C. It is thus recognized that the cubic $BaTiO_3$ core in sample C appears in the DSC curve [Fig. 4(C)]; the cubic phase is certainly retained at temperatures above 130 °C [see Fig. 1(C) and 3(C)].

Dielectric measurements

The temperature dependence of the relative permittivity [$\varepsilon(T)$] of the compact made from sample A[3] is shown in Fig. 5(A) to compare with those of samples B and C. Sample A compact was prepared by HIP sintering to attain 83% theoretical density (7.73 g cm^{-3}). It showed a relatively abrupt dielectric anomaly at 470 °C, due to the t↔c transition as evidenced by HTXRD and DSC, in accordance with the literature.[1]

Sintered compacts of samples B and C were produced at relatively low temperatures of 900 and 800 °C, respectively, without compositional change in the particles. The XRD results after sintering showed no change in the XRD patterns,

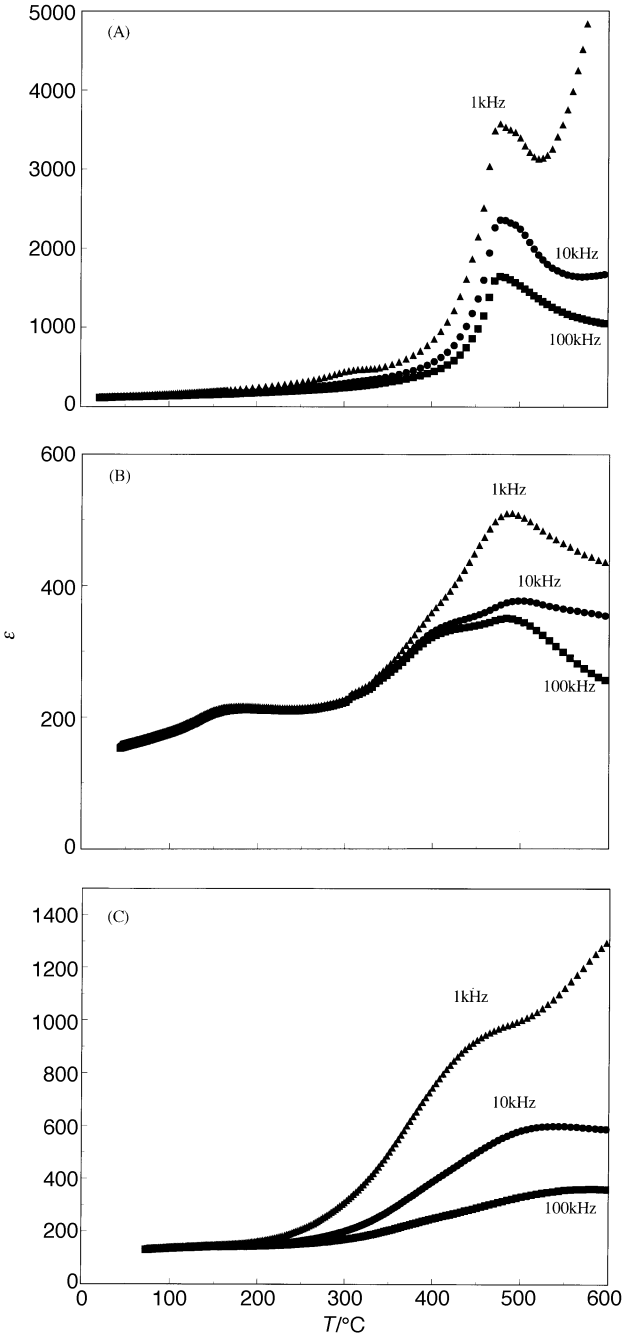

Fig. 5 Temperature dependence of the relative permittivity, $\varepsilon(T)$, for (A) $Ba_{0.13}Pb_{0.87}TiO_3$ solid solution, (B) large composite particles of $BaTiO_3$–$Ba_{1-x}Pb_xTiO_3$ and (C) small composite particles of $BaTiO_3$–$Ba_{1-x}Pb_xTiO_3$ during heating

suggesting that the two phases of $Ba_{1-x}Pb_xTiO_3$ and $BaTiO_3$ were maintained. The apparent bulk densities of the pellets of samples A and B were 4.04 and 4.21 g cm^{-3}, respectively. Fig. 5(B) shows the $\varepsilon(T)$ curves for the sintered compact prepared from sample B. Three frequency-independent permittivity maxima occur at 150, 400 and 480 °C, corresponding to three DSC endotherms [Fig. 4(B)]. The permittivity maximum at 150 °C is due to the t↔c transition of the $BaTiO_3$ core. The second and third maxima are due to the t↔c transition for the $Ba_{1-x}Pb_xTiO_3$ shell with $0.5 \leqslant x \leqslant 0.8$ and $x \approx 0.9$, as determined by HTXRD [Fig. 3(B)]. Although the relative permittivity of the $BaTiO_3$ core is much smaller than that of the covering $Ba_{1-x}Pb_xTiO_3$ shell, the amount of $BaTiO_3$ core in the composite particle is about half of the $Ba_{1-x}Pb_xTiO_3$ shell, according to the X-ray intensity ratio of the cubic 200 peaks at 550 °C [Fig. 3(B)] and the DSC result [Fig. 4(B)].

Each $\varepsilon(T)$ curve for the sintered compact of sample C shows one permittivity maximum [Fig. 5(C)], each maximum temperature shifting towards lower temperature with decreasing frequency. This behaviour is similar to that of lead-based relaxor ferroelectrics, which show a diffuse ferroelectric↔paraelectric transition and frequency dependence of the $\varepsilon(T)$ curve.[9–11] The broad $\varepsilon(T)$ anomaly over a wide temperature range (about 250–500 °C) may be associated with the diffuse t↔c transition of the $Ba_{1-x}Pb_xTiO_3$ component of the composite particles. The continuous rise of the $\varepsilon(T)$ curve above 500 °C at 1 kHz is thought to be related to the increasing dielectric loss and conductivity.

Conclusions

Composite particles of $BaTiO_3$–$Ba_{1-x}Pb_xTiO_3$ were synthesized by molten salt reaction at 600 °C in the $BaTiO_3$–$PbCl_2$ system. The composite particles appear to consist of core–shell $BaTiO_3$–$Ba_{1-x}Pb_xTiO_3$ by XRD and EDXA.

Two sizes of composite $BaTiO_3$–$Ba_{1-x}Pb_xTiO_3$ particles were prepared from $BaTiO_3$ powders of different sizes (0.1 and 0.5 μm) and different molar ratios of $PbCl_2/BaTiO_3$ (1.0 and 0.5). Large composite particles prepared from 0.5 μm $BaTiO_3$ had two x values in $Ba_{1-x}Pb_xTiO_3$ ($0.5 \leqslant x \leqslant 0.8$ and $x \approx 0.9$), while small particles made from 0.1 μm $BaTiO_3$ had $0.4 \leqslant x \leqslant 1.0$. Measurements of the phase transitions in the composite particles by HTXRD and DSC provided these estimated values of x in the $Ba_{1-x}Pb_xTiO_3$ shell.

The $\varepsilon(T)$ curve for a sintered compact fabricated from large composite particles showed three maxima, corresponding to the t↔c transition of $BaTiO_3$, Pb-deficient $Ba_{1-x}Pb_xTiO_3$ and Pb-rich $Ba_{0.1}Pb_{0.9}TiO_3$. A sintered compact prepared from small composite particles exhibited only one maximum with a broad anomaly and frequency dependence which probably arise from the diffuse transition of the $Ba_{1-x}Pb_xTiO_3$ shell.

This work was supported by a Sasakawa Scientific Research Grant from The Japan Science Society and Research Fellowships of the Japan Society for the Promotion of Science for Young Scientists. We are grateful to Mr. Mochizuki and Mr. Sugawara in our Department for the use of the JEOL-2000ES electron microscope and EDX system.

References

1 N. Ichinose and T. Shiosaki, *Electroceramics*, Gihodo, Japan, 1984, pp. 93–99.
2 D. Hennings and G. Rosenstein, *J. Am. Ceram. Soc.*, 1984, **67**, 249.
3 Y. Park and Y. Kim, *J. Mater. Res.*, 1995, **10**, 2770.
4 S. Pathumarak, M. Al-Kahafaji and W. E. Lee, *Br. Ceram. Trans.*, 1994, **93**, 114.
5 G. Shirane and K. Suzuki, *J. Phys. Soc. Jpn.*, 1951, **6**, 274.
6 Y. Ito, S. Shimada and M. Inagaki, *J. Am. Ceram. Soc.*, 1995, **78**, 2695.
7 Y. Ito, S. Shimada and M. Inagaki, *Eur. J. Solid State Inorg. Chem.*, 1995, **32**, 741.
8 G. Shirane and A. Takeda, *J. Phys. Soc. Jpn.*, 1951, **6**, 32.
9 G. A. Smolemskii, V. A. Isupov, A. I. Agranovskaya and S. N. Popov, *Sov. Phys. Solid State (Engl. Transl.)*, 1961, **2**, 2584.
10 T. Tsurumi and F. Uchikoba, *Bull. Ceram. Soc. Jpn.*, 1996, **31**, 128.
11 H. Kanai, O. Furukawa, S. Nakamura and Y. Yamashita, *J. Am. Ceram. Soc.*, 1993, **76**, 454.

Paper 6/05546J; *Received* 8*th August*, 1996